

# Centrosome Size Sets Mitotic Spindle Length in *Caenorhabditis elegans* Embryos

Garrett Greenan,<sup>1,2</sup> Clifford P. Brangwynne,<sup>1,2,3</sup> Steffen Jaensch,<sup>1</sup> Jöbin Gharakhani,<sup>2,3</sup> Frank Jülicher,<sup>2,3,\*</sup> and Anthony A. Hyman<sup>1,2,\*</sup>

<sup>1</sup>Max Planck Institute of Molecular Cell Biology and Genetics, Pfotenhauerstrasse 108, 01307 Dresden, Germany

<sup>2</sup>Physiology Course, Marine Biological Laboratory, 7 MBL Street, Woods Hole, MA 02543, USA

<sup>3</sup>Max Planck Institute for the Physics of Complex Systems, Nöthnitzerstrasse 38, 01187 Dresden, Germany

## Summary

Just as the size of an organism is carefully controlled, the size of intracellular structures must also be regulated. The mitotic spindle is a supramolecular machine that generates the forces which separate sister chromatids during mitosis [1]. Although spindles show little size variation between cells of the same type, spindle length can vary at least 10-fold between different species [2]. Recent experiments on spindle length showed that in embryonic systems spindle length varied with blastomere size [3]. Furthermore, a comparison between two *Xenopus* species showed that spindle length was dependent on some cytoplasmic factor [4]. These data point toward mechanisms to scale spindle length with cell size. Centrosomes play an important role in organizing microtubules during spindle assembly [5]. Here we use *Caenorhabditis elegans* to study the role of centrosomes in setting spindle length. We show that spindle length correlates with centrosome size through development and that a reduction of centrosome size by molecular perturbation reduces spindle length. By systematically analyzing centrosome proteins, we show that spindle length does not depend on microtubule density at centrosomes. Rather, our data suggest that centrosome size sets mitotic spindle length by controlling the length scale of a TPXL-1 gradient along spindle microtubules.

## Results and Discussion

After fertilization of a *Caenorhabditis elegans* oocyte, the zygote undergoes a program of mitotic cell divisions. With each division the cells get smaller due to size constraints imposed by the eggshell. To see how spindle length responded to these changes in cell size, spindles were imaged through the early embryonic divisions. We defined half spindle length as the distance from the center of the centrosome to the center of the chromatin at metaphase, and used  $\gamma$ -tubulin::GFP and histone-H2B::GFP to mark centrosomes and chromatin, respectively. This analysis revealed that spindle length decreased with each mitotic division (Figure 1A), and that there was a strong correlation between spindle length and cell volume (see Figure S1A available online) ( $p < 0.005$ ).

We then looked at how other parameters of the mitotic spindle responded to changes in cell volume through the early

embryonic divisions. No significant correlation was observed between kinetochore amount and cell volume (Figure S1B) ( $p > 0.05$ ), or metaphase plate height and cell volume (Figure S1C) ( $p > 0.05$ ). In contrast, when we quantified centrosome diameter by using a Gaussian fit, we found a highly significant correlation with cell volume (Figure S1D) ( $p < 0.005$ ). Moreover, an examination of the relationship between centrosome diameter and spindle length revealed a strong correlation, using either  $\gamma$ -tubulin::GFP (Figure 1B) ( $p < 0.005$ ) or SPD-5::YFP (Figure S2) ( $p < 0.005$ ) to mark centrosomes.

The correlation we saw between spindle length and centrosome size suggested a mechanism whereby centrosome size could be used to set spindle length. To test this idea, we used RNA interference (RNAi) to reduce centrosome size, and monitored the effect on spindle length. Both RNAi by injection and RNAi by feeding were used in this work (Experimental Procedures). We first used *spd-2(RNAi)* to gradually reduce the size of the centrosomes during the first cell division. SPD-2 is one of the core centrosome components required for the accumulation of all known centrosome components [6, 7], and its depletion from the one-cell embryo results in small immature centrosomes and failed spindle assembly [8, 9]. Although SPD-2 has a role in centriole duplication, it has been shown that centrosomes containing a single centriole nucleate wild-type levels of microtubules [10]. A *spd-2(RNAi)* time course in embryos expressing  $\gamma$ -tubulin::GFP and histone-H2B::GFP did indeed result in progressively smaller centrosomes, and this correlated strongly with a decrease in spindle length (Figure 1C) ( $p < 0.005$ ).

A second method to reduce centrosome size took advantage of our understanding of centriole duplication. A partial RNAi depletion of one of the proteins required for centriole duplication, SAS-4, generates spindles with differently sized centrosomes in the two-cell-stage embryo [11]. We could therefore compare the two half spindle lengths of a bipolar spindle that have differently sized centrosomes. Using  $\gamma$ -tubulin::GFP to mark centrosomes, we analyzed a *sas-4(RNAi)* time course in which the spindles became increasingly asymmetric. Remarkably, we found that as centrosome diameter was reduced, the corresponding half spindle length was also reduced (Figure 1D) ( $p < 0.005$ ). However, above a certain centrosome size, spindles did not increase in length, suggesting an upper limit to spindle length. Taken together, these data show that centrosome size in *C. elegans* embryos can set the length of the mitotic spindle. This also provides a mechanism for the cell to create asymmetric spindles in which the two half spindles are of different lengths. We see this in P<sub>2</sub> spindles in *C. elegans* embryos, but it is also seen in *Drosophila* larval neuroblasts, where the asymmetry of the spindle is thought to determine the asymmetric position of the cleavage furrow [12].

To determine which centrosome components are involved in setting spindle length, we looked for components whose amount at the centrosome scaled directly with spindle length. For each candidate protein, an RNAi time course was performed in a worm strain that expressed a fluorescently tagged version of the protein being targeted. One-cell-stage embryos from an RNAi time course were imaged through the first mitotic division, and then both the amount of GFP protein at the

\*Correspondence: [julicher@pks.mpg.de](mailto:julicher@pks.mpg.de) (F.J.), [hyman@mpi-cbg.de](mailto:hyman@mpi-cbg.de) (A.A.H.)

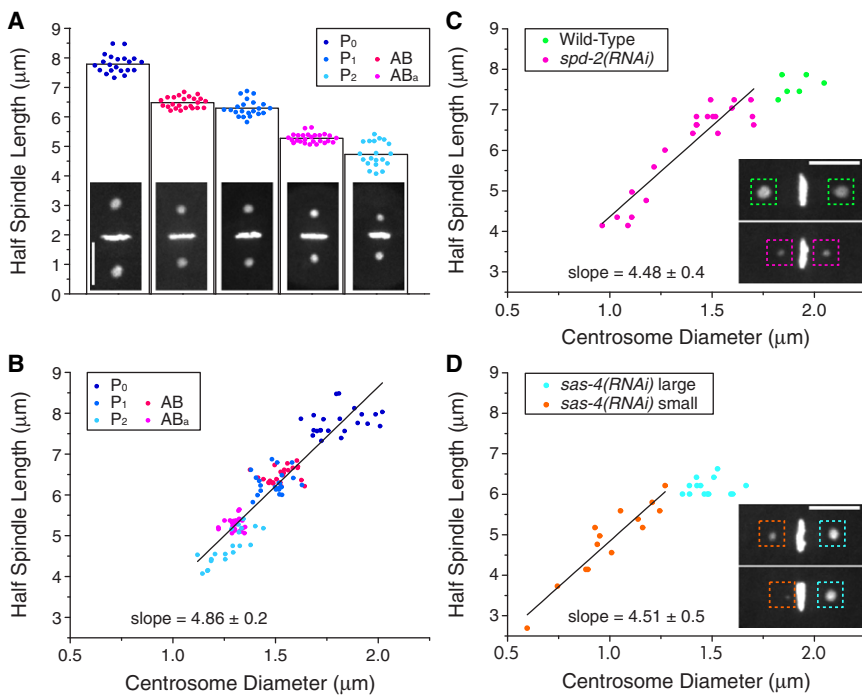


**Figure 1. Centrosome Diameter Correlates with Spindle Length**

(A) Half spindle length decreases through the early mitotic divisions.  $\gamma$ -tubulin::GFP and H2B-histone::GFP embryos were imaged through the early mitotic divisions, and half spindle length was quantified at metaphase. Individual data points are in color; the average is shown as a black column. Insets: representative images. The scale bar represents 10  $\mu$ m.

(B) Centrosome diameter correlates with spindle length through the early mitotic divisions. Centrosome diameter was quantified in  $\gamma$ -tubulin::GFP (and histone-H2B::GFP) worms and showed a strong correlation with half spindle length. Individual data points are shown in color; a linear fit is shown as a black line, slope =  $4.86 \pm 0.2$  (SEM). (C) Reducing centrosome size with *spd-2(RNAi)* results in smaller centrosomes and shorter spindles.  $\gamma$ -tubulin::GFP and H2B-histone::GFP worms were subjected to a *spd-2(RNAi)* time course. Quantification of centrosome diameter and spindle length at metaphase in one-cell-stage embryos showed a strong correlation. Wild-type points are in green, and *spd-2(RNAi)* points are in magenta; a linear fit to the *spd-2(RNAi)* data is shown as a black line, slope =  $4.48 \pm 0.4$  (SEM). Insets: representative images. The scale bar represents 10  $\mu$ m.

(D) *sas-4(RNAi)* asymmetric spindles demonstrate that reducing centrosome size reduces spindle length.

$\gamma$ -tubulin::GFP and H2B-histone::GFP worms were subjected to a *sas-4(RNAi)* time course and asymmetric spindles were generated in the two-cell-stage embryo. Quantification of centrosome diameter and spindle length at metaphase showed a strong correlation. Large centrosomes are in blue, and smaller centrosomes are in orange; a linear fit to the small *sas-4(RNAi)* centrosomes is shown as a black line, slope =  $4.51 \pm 0.5$  (SEM). Inset: representative images. The scale bar represents 10  $\mu$ m.

centrosome and centrosome-to-centrosome distance were quantified at metaphase.

We first investigated the role of  $\gamma$ -tubulin, a centrosome protein that is part of the complex required for efficient

microtubule nucleation and organization [13]. After 12 hr of  *$\gamma$ -tubulin(RNAi)*, ~20% of wild-type  $\gamma$ -tubulin::GFP protein levels remain at centrosomes, but neither spindle length (Figure 2A) nor centrosome diameter (data not shown) are

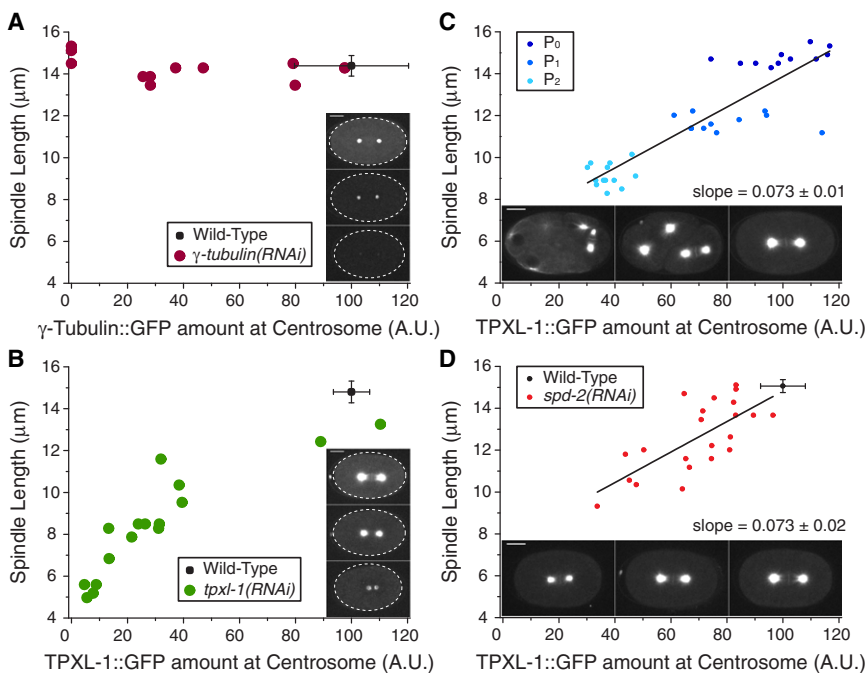


**Figure 2. TPXL-1 Amounts at the Centrosome Are Proportional to Spindle Length**

(A) A  *$\gamma$ -tubulin(RNAi)* time course has no effect on spindle length. Decreasing the amount of  $\gamma$ -tubulin::GFP with  *$\gamma$ -tubulin(RNAi)* had no effect on spindle length. For wild-type,  $n = 4$  P<sub>0</sub> embryos,  $\gamma$ -tubulin::GFP fluorescence amount 100 A.U.  $\pm$  20, spindle length 14.39  $\mu$ m  $\pm$  0.5, and errors are SD. The embryo boundary is indicated with a dashed line.

(B) A *tpxl-1(RNAi)* time course has a strong effect on spindle length. Decreasing the amount of TPXL-1::GFP with *tpxl-1(RNAi)* depleted TPXL-1, and this reduced spindle length. For wild-type,  $n = 4$  P<sub>0</sub> embryos, TPXL-1::GFP fluorescence amount 100 A.U.  $\pm$  6, spindle length 14.80  $\mu$ m  $\pm$  0.5, and errors are SD. The embryo boundary is indicated with a dashed line.

(C) TPXL-1::GFP amounts at the centrosome correlate with spindle length through the early P lineage divisions. TPXL-1::GFP-expressing worms were imaged through development, and TPXL-1 amounts at the centrosome were quantified for cells in the P lineage (P<sub>0</sub>, P<sub>1</sub>, P<sub>2</sub>). Individual data points are shown in color; a linear fit is shown as a black line, slope =  $0.073 \pm 0.01$  (SEM). (D) A *spd-2(RNAi)* time course in TPXL-1::GFP embryos shows that TPXL-1 amounts at the centrosome correlate with spindle length.

Decreasing centrosome size with *spd-2(RNAi)* resulted in shorter spindles and in reduced amounts of TPXL-1::GFP at centrosomes. For wild-type,  $n = 4$  P<sub>0</sub> embryos, TPXL-1::GFP fluorescence amount 100 A.U.  $\pm$  8, spindle length 15.06  $\mu$ m  $\pm$  0.3, and errors are SD. Individual *spd-2(RNAi)* data points are shown in red; a linear fit is shown as a black line, slope =  $0.073 \pm 0.02$  (SEM). Insets: representative images. The scale bars represent 10  $\mu$ m.

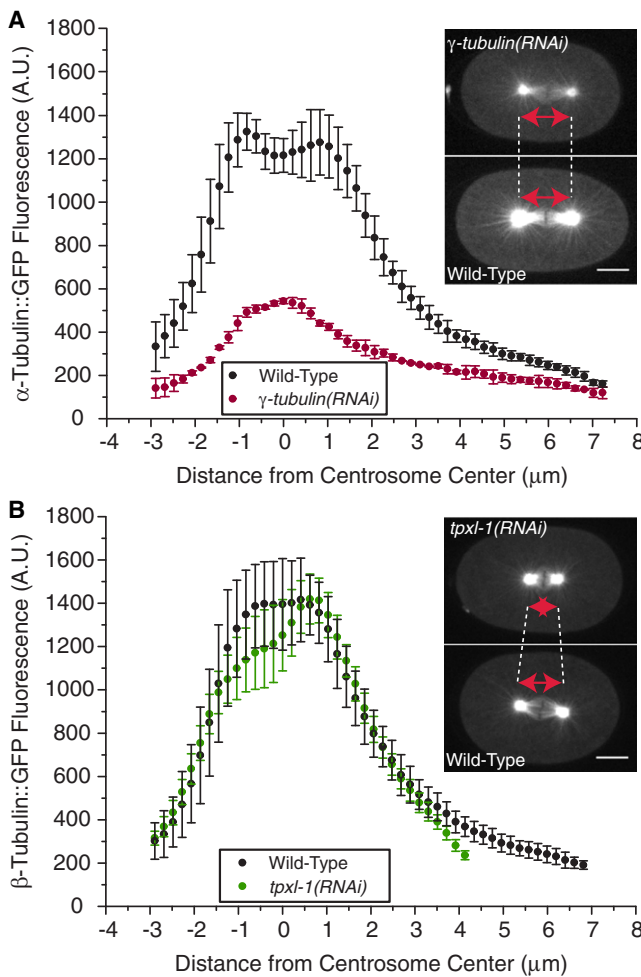


**Figure 3. Microtubule Density Does Not Correlate with Spindle Length**  
(A)  $\gamma$ -tubulin(RNAi) reduces spindle microtubule density, but spindle length is unaffected. The distribution of  $\alpha$ -tubulin::GFP as a function of distance from the center of the centrosome was determined for wild-type ( $n = 8$ ) and  $\gamma$ -tubulin(RNAi) ( $n = 4$ ) P<sub>0</sub> half spindles. Error bars are SD. Inset: representative images. The scale bar represents 10  $\mu$ m.  
(B)  $tpxl-1$ (RNAi) results in shorter spindles but does not affect spindle microtubule density. The distribution of  $\beta$ -tubulin::GFP as a function of distance from the center of the centrosome was determined for wild-type ( $n = 10$ ) and  $tpxl-1$ (RNAi) ( $n = 10$ ) P<sub>0</sub> half spindles. Error bars are SD. Inset: representative images. The scale bar represents 10  $\mu$ m.

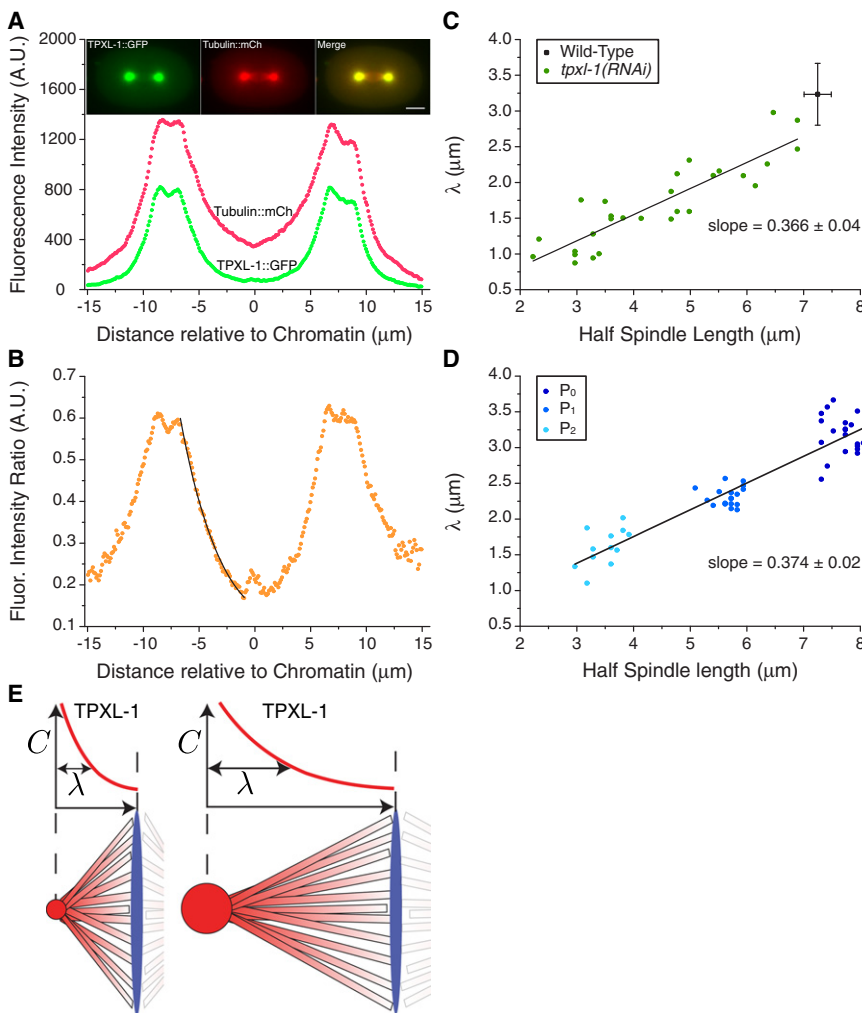
significantly affected. At 22 hr of  $\gamma$ -tubulin(RNAi), we could no longer detect  $\gamma$ -tubulin::GFP at the centrosome; under these RNAi conditions, spindle length remained unchanged (Figure 2A). It has previously been shown that functional spindles fail to assemble after long  $\gamma$ -tubulin(RNAi) treatment [14, 15]. To rule out the possibility that  $\gamma$ -tubulin::GFP was preferentially depleted over endogenous  $\gamma$ -tubulin during RNAi, we confirmed these results by using a  $\gamma$ -tubulin antibody (Figure S3A). Thus,  $\gamma$ -tubulin levels at the centrosome did not correlate with spindle length, suggesting that microtubule number is not a major factor in determining spindle length. Consistent with this, after 22 hr of  $\gamma$ -tubulin(RNAi), there was a significant reduction in microtubule density within the spindle, but spindle length was unchanged (Figure 3A). This confirmed that  $\gamma$ -tubulin is required for microtubule nucleation and organization at centrosomes, but that the number of microtubules is not directly correlated with spindle length.

We next examined the contribution of TAC-1, a protein that influences microtubule growth rates together with its binding partner ZYG-9, a TOG/XMAP215-related protein [16]. Depletion of either TAC-1 or ZYG-9 results in severely reduced microtubule growth rates [10]. After 24 hr of (*tac-1*)RNAi, the TAC-1::GFP signal was not detectable, but this had only a small effect on spindle length (~15% reduction) (Figure S3B). Similar results were seen after RNAi of ZYG-9 (data not shown). The depletion of KLP-7, a member of the kinesin-13 family of depolymerizing kinesins, results in an increase of centrosomal microtubules [10, 17]. We used RNAi to deplete KLP-7 in a  $\gamma$ -tubulin::GFP, histone-H2B::GFP worm strain (see Experimental Procedures). As in the *tac-1*(RNAi) experiment, *kfp-7*(RNAi) showed only a small reduction in spindle length (~15% reduction) (Figure S3C). Surprisingly, therefore, neither the number of microtubules at centrosomes nor their growth rate had a significant effect on spindle length in the one-cell *C. elegans* embryo.

One protein complex that is known to play a role in spindle assembly is the TPXL-1/Aurora A kinase complex [18, 19]. TPXL-1 is the *C. elegans* homolog of TPX2 and has been shown to bind, activate, and target Aurora A kinase to microtubules [19]. Abolition of the interaction between TPXL-1 and Aurora A results in centrosomes collapsing onto the chromatin during mitosis [19]. Furthermore, TPXL-1 is seen on both centrosomes and spindles during mitosis, and was therefore a good candidate to link centrosome size and spindle length. We tested the contribution of TPXL-1 to spindle length by performing a *tpxl-1*(RNAi) time course in a TPXL-1::GFP line in which TPXL-1::GFP was previously shown to be functional [19]. We found that after just 6 hr of *tpxl-1*(RNAi), less than 10% of wild-type TPXL-1::GFP remained at centrosomes. Under these conditions, spindle length was greatly reduced (Figure 2B). The *tpxl-1*(RNAi) time course showed a strong correlation between the amount of TPXL-1::GFP at the centrosome and spindle length. We found a similar reduction in spindle length after *tpxl-1*(RNAi) in a worm strain expressing  $\gamma$ -tubulin::GFP and histone-H2B::GFP, but centrosome diameter, as marked by  $\gamma$ -tubulin::GFP, remained unchanged (Figure S3D). These experiments showed that TPXL-1 is involved in setting spindle length, but not by controlling centrosome size.

Consistent with a role for TPXL-1, we found that in untreated worms, centrosomal TPXL-1::GFP levels correlated with spindle length through development (Figure 2C) ( $p < 0.005$ ). We also examined embryos expressing TPXL-1::GFP that were subjected to a *spd-2*(RNAi) time course to reduce centrosome size. When TPXL-1::GFP levels were plotted against spindle length, they were strongly correlated (Figure 2D) ( $p < 0.005$ ). Moreover, the data from both these experiments were remarkably similar. Taken together, this indicates that TPXL-1 amounts at the centrosome are proportional to spindle length, providing further support for a central role of TPXL-1 in regulating spindle length.

To study how TPXL-1 controls spindle length, we first looked at the relationship between microtubule density and TPXL-1 levels. We quantified the density of microtubules for both wild-type and *tpxl-1*(RNAi) spindles by using a  $\beta$ -tubulin::GFP strain that fluorescently labels microtubules. We found little difference in microtubule density between wild-type spindles and *tpxl-1*(RNAi) spindles, whose length was 60% of wild-type (Figure 3B). This indicates that TPXL-1 does not influence microtubule density, but rather must act by some other mechanism.



In addition to its localization to centrosomes, TPXL-1 also localizes to spindles, decreasing in intensity along the spindle from the centrosome to the chromatin (Figure 4A). To see whether the TPXL-1 intensity simply reflected the tubulin intensity, we calculated the ratio of TPXL-1 to tubulin intensity along spindles, which we call  $C$ . We found that  $C$  formed a gradient along the spindle microtubules, with a maximum at the centrosome, decaying toward the kinetochores (Figure 4B). A similar gradient was observed for Aurora A kinase (Figure S4). The TPXL-1 gradient could be fit by an exponential function of the form  $C \sim e^{-x/\lambda}$ , where  $x$  is the distance from the centrosome along the spindle, and  $\lambda$  is the characteristic length scale of the gradient (see Experimental Procedures). A *tpxl-1(RNAi)* time course in TPXL-1::GFP-expressing and tubulin::mCherry-expressing worms showed that  $\lambda$  decreased as spindle length decreased (Figure 4C) ( $p < 0.005$ ). Similar changes in  $\lambda$  were seen as spindles decreased in size through early development (Figure 4D) ( $p < 0.005$ ); the data exhibited a slope similar to that seen in the *tpxl-1(RNAi)* time course. A small population of TPXL-1 also accumulated at kinetochores, but this TPXL-1 population did not show any consistent relationship with spindle length (data not shown). Together, these data show that TPXL-1 decreases away from the centrosome faster than microtubules, and that the length scale of the TPXL-1 gradient along spindle microtubules correlates strongly with the length of the spindle.

Figure 4. The TPXL-1 Gradient Decay Length along Microtubules Scales with Spindle Length (A) TPXL-1::GFP and tubulin::mCherry distribution along a metaphase spindle. A line scan was used to look at the distribution of TPXL-1::GFP and tubulin::mCherry as a function of distance from the center of the chromatin. Inset: representative images. The scale bar represents 10  $\mu\text{m}$ . (B) TPXL-1::GFP per microtubule shown as the ratio of TPXL-1::GFP fluorescence to tubulin::mCherry fluorescence. The profile between the centrosome and the chromatin was well fit by an exponential function ( $C(x) = Ae^{-x/\lambda} + Be^{+x/\lambda}$ ; black line), characterized by a decay length,  $\lambda = 3.967$  (additional parameters:  $A = 0.116$ ,  $B = 0.0246$ ). (C) The decay length,  $\lambda$ , of TPXL-1::GFP (determined as shown in B) changes with *tpxl-1(RNAi)*. Decreasing the amount of TPXL-1 by using *tpxl-1(RNAi)* resulted in shorter spindles and in a reduced decay length  $\lambda$  of the TPXL-1::GFP/tubulin::mCherry profile. For wild-type,  $n = 8$   $P_0$  half spindles, half spindle length is  $7.25 \mu\text{m} \pm 0.2$ ,  $\lambda$  is  $3.23 \mu\text{m} \pm 0.4$ , and errors are SD. Individual *tpxl-1(RNAi)* data points are shown in green; a linear fit is shown as a black line, slope =  $0.366 \pm 0.04$  (SEM). (D) The TPXL-1::GFP decay length,  $\lambda$ , decreases as spindle length decreases during development. TPXL-1::GFP-expressing and tubulin::mCherry-expressing worms were imaged through development, and the TPXL-1 decay rate  $\lambda$  and half spindle length were quantified for cells in the P lineage ( $P_0$ ,  $P_1$ ,  $P_2$ ). Individual data points are shown in color; a linear fit is shown as a black line, slope =  $0.374 \pm 0.02$  (SEM). (E) Schematic illustrating how the characteristic length scale,  $\lambda$ , of the TPXL-1 gradient sets spindle length.

The change in the shape of the TPXL-1 gradient as spindle length changes suggests a physical picture in which the characteristic length scale of the TPXL-1 gradient,  $\lambda$ , sets spindle length (Figure 4E). In meiotic systems, gradients around chromatin are thought to be key to limiting spindle length [20]. Such mechanisms are reminiscent of developmental morphogen gradients, which provide positional information in tissues [21, 22]. We do not know how the decay length of the TPXL-1 gradient is set. In one simple scenario, TPXL-1 binds to spindle microtubules at the centrosome and diffuses along microtubules from which it can detach. A TPXL-1 gradient of the form  $C \sim e^{-x/\lambda}$  is then naturally generated, where the TPXL-1 decay length is set by the diffusion coefficient,  $D$ , and the detachment rate,  $k$  ( $\lambda = (D/k)^{1/2}$ ). The fact that the decay length of TPXL-1 apparently depends on TPXL-1 levels at the centrosome suggests that the reaction diffusion system must exhibit some nonlinear, collective behavior. Examples include a diffusion coefficient or a microtubule detachment rate that depends on TPXL-1 levels; a more complicated mechanism involving active transport or an Aurora A kinase feedback loop could also be at work (see Supplemental Discussion).

Our data show that cells set spindle length in blastomeres at least in part by controlling the size of the centrosomes. Furthermore, our experiments suggest that centrosome size sets the length of spindles by determining the amount of

TPXL-1 on spindles. This is consistent with previous results in human cells [18], indicating that TPXL-1 and related proteins may have a conserved role in setting mitotic spindle length. We do not know the molecular mechanisms by which TPXL-1 and related proteins set spindle length. A TPXL-1/Aurora A kinase gradient could be read by kinetochores, perhaps by modulating the detachment rate of kinetochore microtubules. Another possibility is that the local concentration of TPXL-1/Aurora A kinase on a microtubule sets a balance point between microtubule growth and shrinkage. In this case, the problem of setting the size of the spindle is simplified to that of setting the length of individual spindle microtubules [23, 24]. Elucidating the underlying mechanism of how a cell sets centrosome size, and how this in turn is used to set the length scale of a TPXL-1 gradient and spindle length, will be interesting directions for future research.

### Experimental Procedures

#### Worm Strains and RNA Interference

Maintenance of *C. elegans* worm strains was carried out according to standard protocols [25]. A complete list of worm strains used in this work can be found in Supplemental Information. Worms were subjected to both RNAi by injection, and RNAi by feeding as previously described [26, 27]. The RNAi method used for each gene, as well as the region targeted is indicated in Supplemental Experimental Procedures.

#### Imaging

For live imaging, worms were dissected on glass coverslips in M9 buffer and then mounted on 2% agar pads. Live-cell imaging was conducted at 20°C. Single-color (GFP or YFP) imaging was carried out on a spinning disc system consisting of a Zeiss Axio Imager Z1 microscope body, a Yokagawa spinning disc head, a Melles Griot 488 nm 43 series argon ion laser, and a Hamamatsu Orca ER 12-bit digital camera. The lens used was a C-Apochromat, 63×/1.2 W Korr UV-vis-IR from Zeiss. Two-color imaging (GFP and mCherry) was carried out by widefield microscopy with a Zeiss Axioplan 2 microscope body and a Hamamatsu Orca I CCD camera. The lens used was a Plan-Apochromat, 63×/1.4 Oil DIC from Zeiss. MetaMorph was used to control the microscopes and acquire images. Fixed images were acquired on a widefield Delta Vision microscope from Applied Precision, with a Roper Scientific CoolSNAP camera and a Plan-Apo 60×/1.42 lens from Olympus. The microscope was controlled by SoftWorx software. Raw images were computationally deconvolved before image analysis and then projected for presentation.

#### Image Analysis

Quantification of cell volume, spindle length, kinetochore amount, and metaphase plate height, as well as line scans quantifying the distribution of tubulin, TPXL-1, and Aurora A kinase along the spindle, were all conducted in ImageJ. Matlab was used to fit a Gaussian distribution to the centrosome, allowing quantification of both centrosome diameter (full width at half maximum) and centrosomal protein amount. A more detailed description of the fluorescent markers used and the analysis can be found in Supplemental Experimental Procedures.

#### Line Fitting, Curve Fitting, and Statistics

Following line fitting, linear regression was used to determine whether there was a significant correlation between parameters. A Welch's *t* test was used to determine whether there was a significant difference between two sets of measurements. Formulae used for both can be found in Supplemental Information. For the spindle gradients, Matlab was used to fit the function  $C(x) = Ae^{-x/\lambda} + Be^{+x/\lambda}$  to the data corresponding to the region between the centrosome and the chromatin. Details of the curve-fitting procedure can be found in the Supplemental Experimental Procedures.

#### Supplemental Information

Supplemental Information includes four figures, Supplemental Discussion, and Supplemental Experimental Procedures, and can be found with this article online at doi:10.1016/j.cub.2009.12.050.

### Acknowledgments

The authors thank T. Davis, A. Desai, M. Srayko, C. Cowan, T. Müller-Reichert, and M. Mayer for comments on the manuscript, and past and present members of the Hyman lab for helpful suggestions and experimental advice.

Received: August 28, 2009

Revised: December 15, 2009

Accepted: December 17, 2009

Published online: February 4, 2010

### References

1. Dumont, S., and Mitchison, T.J. (2009). Force and length in the mitotic spindle. *Curr. Biol.* 19, R749–R761.
2. Karsenti, E., and Vernos, I. (2001). The mitotic spindle: A self-made machine. *Science* 294, 543–547.
3. Wuhr, M., Chen, Y., Dumont, S., Groen, A.C., Needleman, D.J., Salic, A., and Mitchison, T.J. (2008). Evidence for an upper limit to mitotic spindle length. *Curr. Biol.* 18, 1256–1261.
4. Brown, K.S., Blower, M.D., Maresca, T.J., Grammer, T.C., Harland, R.M., and Heald, R. (2007). *Xenopus tropicalis* egg extracts provide insight into scaling of the mitotic spindle. *J. Cell Biol.* 176, 765–770.
5. Wittmann, T., Hyman, A., and Desai, A. (2001). The spindle: A dynamic assembly of microtubules and motors. *Nat. Cell Biol.* 3, E28–E34.
6. Boxem, M., Maliga, Z., Klitgord, N., Li, N., Lemmens, I., Mana, M., de Lichtervelde, L., Mul, J.D., van de Peut, D., Devos, M., et al. (2008). A protein domain-based interactome network for *C. elegans* early embryogenesis. *Cell* 134, 534–545.
7. Oegema K., and Hyman A.A. (2006). Cell division. In *WormBook*, The *C. elegans* Research Community, ed. 10.1895/wormbook.1.72.1, <http://www.wormbook.org>.
8. Kemp, C.A., Kopish, K.R., Zipperlen, P., Ahringer, J., and O'Connell, K.F. (2004). Centrosome maturation and duplication in *C. elegans* require the coiled-coil protein SPD-2. *Dev. Cell* 6, 511–523.
9. Pelletier, L., Ozlu, N., Hannak, E., Cowan, C., Habermann, B., Ruer, M., Muller-Reichert, T., and Hyman, A.A. (2004). The *Caenorhabditis elegans* centrosomal protein SPD-2 is required for both pericentriolar material recruitment and centriole duplication. *Curr. Biol.* 14, 863–873.
10. Srayko, M., Kaya, A., Stamford, J., and Hyman, A.A. (2005). Identification and characterization of factors required for microtubule growth and nucleation in the early *C. elegans* embryo. *Dev. Cell* 9, 223–236.
11. Kirkham, M., Muller-Reichert, T., Oegema, K., Grill, S., and Hyman, A.A. (2003). SAS-4 is a *C. elegans* centriolar protein that controls centrosome size. *Cell* 112, 575–587.
12. Rebollo, E., Sampaio, P., Januschke, J., Llamazares, S., Varmark, H., and Gonzalez, C. (2007). Functionally unequal centrosomes drive spindle orientation in asymmetrically dividing *Drosophila* neural stem cells. *Dev. Cell* 12, 467–474.
13. Oakley, B.R., Oakley, C.E., Yoon, Y., and Jung, M.K. (1990).  $\gamma$ -tubulin is a component of the spindle pole body that is essential for microtubule function in *Aspergillus nidulans*. *Cell* 61, 1289–1301.
14. Hannak, E., Oegema, K., Kirkham, M., Gonczy, P., Habermann, B., and Hyman, A.A. (2002). The kinetically dominant assembly pathway for centrosomal asters in *Caenorhabditis elegans* is  $\gamma$ -tubulin dependent. *J. Cell Biol.* 157, 591–602.
15. Strome, S., Powers, J., Dunn, M., Reese, K., Malone, C.J., White, J., Seydoux, G., and Saxton, W. (2001). Spindle dynamics and the role of  $\gamma$ -tubulin in early *Caenorhabditis elegans* embryos. *Mol. Biol. Cell* 12, 1751–1764.
16. Srayko, M., Quintin, S., Schwager, A., and Hyman, A.A. (2003). *Caenorhabditis elegans* TAC-1 and ZYG-9 form a complex that is essential for long astral and spindle microtubules. *Curr. Biol.* 13, 1506–1511.
17. Schlaitz, A.L., Srayko, M., Dammermann, A., Quintin, S., Wielsch, N., MacLeod, I., de Robillard, Q., Zinke, A., Yates, J.R., 3rd, Muller-Reichert, T., et al. (2007). The *C. elegans* RSA complex localizes protein phosphatase 2A to centrosomes and regulates mitotic spindle assembly. *Cell* 128, 115–127.
18. Bird, A.W., and Hyman, A.A. (2008). Building a spindle of the correct length in human cells requires the interaction between TPX2 and Aurora A. *J. Cell Biol.* 182, 289–300.

19. Ozlu, N., Srayko, M., Kinoshita, K., Habermann, B., O'Toole, E.T., Muller-Reichert, T., Schmalz, N., Desai, A., and Hyman, A.A. (2005). An essential function of the *C. elegans* ortholog of TPX2 is to localize activated Aurora A kinase to mitotic spindles. *Dev. Cell* 9, 237–248.
20. Hyman, A.A., and Karsenti, E. (1996). Morphogenetic properties of microtubules and mitotic spindle assembly. *Cell* 84, 401–410.
21. Ben-Zvi, D., Shilo, B.Z., Fainsod, A., and Barkai, N. (2008). Scaling of the BMP activation gradient in *Xenopus* embryos. *Nature* 453, 1205–1211.
22. Kicheva, A., Pantazis, P., Bollenbach, T., Kalaidzidis, Y., Bittig, T., Julicher, F., and Gonzalez-Gaitan, M. (2007). Kinetics of morphogen gradient formation. *Science* 315, 521–525.
23. Goshima, G., Wollman, R., Stuurman, N., Scholey, J.M., and Vale, R.D. (2005). Length control of the metaphase spindle. *Curr. Biol.* 15, 1979–1988.
24. Varga, V., Helenius, J., Tanaka, K., Hyman, A.A., Tanaka, T.U., and Howard, J. (2006). Yeast kinesin-8 depolymerizes microtubules in a length-dependent manner. *Nat. Cell Biol.* 8, 957–962.
25. Brenner, S. (1974). The genetics of *Caenorhabditis elegans*. *Genetics* 77, 71–94.
26. Kamath, R.S., Martinez-Campos, M., Zipperlen, P., Fraser, A.G., and Ahringer, J. (2001). Effectiveness of specific RNA-mediated interference through ingested double-stranded RNA in *Caenorhabditis elegans*. *Genome Biol.* 2, RESEARCH0002.
27. Sonnichsen, B., Koski, L.B., Walsh, A., Marschall, P., Neumann, B., Brehm, M., Alleaume, A.M., Artelt, J., Bettencourt, P., Cassin, E., et al. (2005). Full-genome RNAi profiling of early embryogenesis in *Caenorhabditis elegans*. *Nature* 434, 462–469.